MOLECULAR AND CELLULAR BIOLOGY, Dec. 1996, p. 6783–6793 Vol. 16, No. 12
0270-7306/96/$04.00+0

Dual Requirement for the Yeast *MMS19* Gene in DNA Repair and RNA Polymerase II Transcription

SCOTT LAUDER,[1] MICHAEL BANKMANN,[2]† SAMI N. GUZDER,[1] PATRICK SUNG,[1] LOUISE PRAKASH,[1,2] AND SATYA PRAKASH[1,2]*

Sealy Center for Molecular Science, University of Texas Medical Branch, Galveston, Texas,[1] and University of Rochester, Rochester, New York[2]

Received 18 June 1996/Returned for modification 11 September 1996/Accepted 25 September 1996

Genetic and biochemical studies of *Saccharomyces cerevisiae* have indicated the involvement of a large number of protein factors in nucleotide excision repair (NER) of UV-damaged DNA. However, how *MMS19* affects this process has remained unclear. Here, we report on the isolation of the *MMS19* gene and the determination of its role in NER and other cellular processes. Genetic and biochemical evidence indicates that besides its function in NER, *MMS19* also affects RNA polymerase II (Pol II) transcription. *mms19*Δ cells do not grow at 37°C, and mutant extract exhibits a thermolabile defect in Pol II transcription. Thus, Mms19 protein resembles TFIIH in that it is required for both transcription and DNA repair. However, addition of purified Mms19 protein does not alleviate the transcriptional defect of the *mms19*Δ extract, nor does it stimulate the incision of UV-damaged DNA reconstituted from purified proteins. Interestingly, addition of purified TFIIH corrects the transcriptional defect of the *mms19*Δ extract. Mms19 is, however, not a component of TFIIH or of Pol II holoenzyme. These and other results suggest that Mms19 affects NER and transcription by influencing the activity of TFIIH as an upstream regulatory element. It is proposed that mutations in the human *MMS19* counterpart could result in syndromes in which both NER and transcription are affected.

In eukaryotes, nucleotide excision repair (NER) of DNA damaged by UV and by other agents that distort the DNA helix is a highly complex process that involves a large number of protein factors. A defect in NER in humans results in xeroderma pigmentosum (XP), and deficiency in NER occurs in patients with trichothiodystrophy and Cockayne's syndrome. Persons with XP are highly sensitive to the UV component of the solar spectrum, and they have an ~1,000-fold-elevated incidence of skin cancers that include basal cell carcinomas, squamous cell carcinomas, and melanomas. XP cells are hypermutable by UV and by UV-mimetic DNA-damaging agents. Mutagenic bypass of unexcised UV lesions during replication gives rise to hypermutability, which is the underlying cause of skin cancers in individuals with XP. Seven XP complementation groups, A through G, have been identified by cell fusion studies (22).

Genetic studies with the yeast *Saccharomyces cerevisiae* have implicated 11 genes in NER. Mutations in seven of these genes, *RAD1*, *RAD2*, *RAD3*, *RAD4*, *RAD10*, *RAD14*, and *RAD25*, cause extreme UV sensitivity and a defect in the incision step of NER. Mutations in three genes, *RAD7*, *RAD16*, and *RAD23*, confer moderate UV sensitivity, and these mutations result in a lower degree of NER defectiveness than do mutations in genes of the first group (reviewed in reference 31). The *MMS19* gene was initially identified in a screen for mutations that render cells sensitive to the alkylating agent methyl methanesulfonate (MMS) (29). Interestingly, the *mms19-1* mutation thus identified also confers sensitivity to UV and DNA-cross-linking agents, and the removal of UV damage and the nicking of DNA containing interstrand cross-links are severely impaired by this mutation (25, 30), indicating that this mutation impairs the incision step of NER. As is characteristic of NER-defective mutants, the frequency of UV-induced mutations is greatly elevated in the *mms19-1* mutant (30).

Various Rad proteins have been purified, and determination of their biochemical activities has helped clarify their roles in dual incision of UV-damaged DNA. Rad14 is a zinc metalloprotein that binds damaged DNA (14). The Rad1-Rad10 protein complex has a single-stranded DNA endonuclease activity (42, 44). More recently, we have shown that Rad14, Rad1, and Rad10 exist in vivo in a ternary complex which we have designated nucleotide excision repair factor 1 (NEF1) (16); the association with Rad14 provides a mechanism for targeting the Rad1-Rad10 nuclease to the damage site. Rad2 also is a single-stranded DNA endonuclease (17). The Rad4 and Rad23 proteins exist in a tight complex in vivo; however, no biochemical activities have yet been assigned to either of these proteins (11). Rad23 bears a ubiquitin-like domain at its amino terminus, and this domain is important for its function in NER (45). The involvement of Rad23 in the assembly of NER factors (10) has suggested a role for the Rad4-Rad23 complex (NEF2) in assembling the NER machinery at the damage site.

Besides their NER function, the *RAD3* and *RAD25* genes are essential for cell viability because of their requirement in RNA polymerase II (Pol II) transcription (12, 13, 32). Both Rad3 and Rad25 possess single-stranded-DNA-dependent ATPase and DNA helicase activities (13, 39–41). The DNA helicase activity of Rad25 is essential for both NER and Pol II transcription (13, 38), whereas the DNA helicase activity of Rad3 is essential for NER but dispensable for Pol II transcription (38, 39). *XPD*, the human homolog of *RAD3*, also encodes a DNA helicase (37). Interestingly, the XPD Arg-48 mutant protein, which carries a mutation in the DNA helicase domain, restores viability to the *rad3* null mutant, indicating that like that of Rad3, the DNA helicase activity of XPD is dispensable

* Corresponding author. Mailing address: Sealy Center for Molecular Science, University of Texas Medical Branch, 6.104 Medical Research Building, Galveston, TX 77555-1061. Phone: (409) 747-8602. Fax: (409) 747-8608. Electronic mail address: sprakash@scms.utmb.edu.

† Present address: Hoechst Aktiengesellschaft Patent- und Lizenzabteilung, D-65926 Frankfurt am Main, Germany.

in Pol II transcription (15). Rad3 and Rad25 are subunits of the Pol II transcription factor TFIIH, which contains four additional subunits, p38, p55, Ssl1, and Tfb1 (7, 11). These last four subunits can be purified as a separate entity which we have designated TFIIH-incomplete or TFIIHi (38). Neither TFIIHi nor a mixture of Rad3 and Rad25 proteins has any NER activity, but TFIIH fully active in NER can be reconstituted from TFIIHi, Rad3, and Rad25 proteins (38). These studies have provided direct evidence that, in addition to Rad3 and Rad25 proteins, TFIIHi is indispensable for the incision of UV-damaged DNA.

The incision step of NER has been reconstituted from a combination of purified Rad14, the Rad4-Rad23 complex, replication protein A, the six-subunit TFIIH, the Rad1-Rad10 complex, and Rad2 (11, 38). These factors are all indispensable for incision, indicating that they represent the minimal set of protein factors required for this reaction. Incision in the reconstituted system is strictly dependent on ATP, which cannot be replaced by the nonhydrolyzable analog adenosine 5′-*O*-(3-thiotriphosphate) (ATPγS). At the expense of ATP hydrolysis, the combined helicase function of Rad3 and Rad25 proteins in TFIIH presumably creates an unwound DNA structure (38) for dual incision by the Rad1-Rad10 and Rad2 endonucleases 5′ and 3′ to the DNA lesion, respectively (2, 18). NER is highly conserved between *S. cerevisiae* and humans, and a combination of corresponding human proteins results in dual incision of damaged DNA (26, 27).

Since the Rad7, Rad16, and Mms19 proteins have not yet been purified, the manner in which these proteins affect damage-specific incision is not clear at present. To elucidate the molecular role of Mms19, we have cloned the *MMS19* gene and determined the effect of a null mutation (*mms19*Δ) on various biological processes. Interestingly, characterization of the *mms19*Δ mutation has revealed a dual involvement of Mms19 protein in NER and Pol II transcription. Furthermore, our results suggest that Mms19 protein does not participate directly in NER or transcription but that it exerts its biological effects by influencing the activity of TFIIH and possibly other DNA repair and transcription factors. Thus, *MMS19* represents a novel, multifunctional gene whose activity is required upstream of DNA repair reactions and Pol II transcription. We discuss our findings in relation to human genetic diseases in which both NER and transcription are affected.

MATERIALS AND METHODS

Strains and media. *Escherichia coli* DH5α was used for propagation of all plasmids and color selection of plasmid derivatives of YEplac195, YCplac33, YIplac211, and pUC vectors. *E. coli* JM101 was used for propagation of M13 derivatives.

Yeast extract-peptone-dextrose (YPD), synthetic complete, and sporulation media were prepared as described elsewhere (36). *E. coli* strains were cultured in LB, YT, or M9 medium as described elsewhere (24).

Vectors and plasmids. YEp24 (5) and YEplac195 (9) are high-copy-number plasmids that contain the yeast 2μm origin of replication. YCplac33 is a low-copy-number vector containing the yeast *CEN4* and *ARS1* sequences. The integrating vector YIplac211 is maintained in *S. cerevisiae* only by homologous integration into the genome (9). In addition, plasmids YEplac195, YCplac33, and YIplac211 have the multicloning site of pUC19, the yeast *URA3* sequence with the *Pst*I site removed, and the *lacZ* system of the pUC plasmids, allowing convenient color selection for DNA inserts.

For overproduction of Mms19 protein in *S. cerevisiae*, an *Eco*RI site was introduced 10 nucleotides upstream of the initiating ATG codon of *MMS19* by site-directed mutagenesis. A 3.4-kb fragment containing this 5′ *Eco*RI site and the 3′ *Eco*RI site at the end of the *MMS19* sequence shown in Fig. 1 was blunt ended and then ligated into the blunt-ended *Bgl*II site of plasmid pPE280 (21), generating plasmid pMMS19.7. This results in the *MMS19* gene being expressed under the control of a *GAL1-10-PGK* hybrid promoter.

Transformation and other procedures. Yeast cells were transformed by the lithium acetate method (19). Transformation of *E. coli* cells, electrophoresis of DNA, plasmid preparations, and Southern hybridizations were performed as described elsewhere (24), whereas DNA fragments were cloned into vector plasmids by the low-melting-point agarose method (20).

Isolation of the *MMS19* gene. To enhance its UV sensitivity, the *mms19-1* mutation was combined with the *rad5-1* mutation, which impairs *RAD6*-dependent DNA repair processes. The *mms19-1 rad5-1 ura3-52* strain BM1034-2C (*MAT*α *mms19-1 rad5-1 his3-*Δ*1 trp1-289 leu2-3,112 ura3-52*) was transformed to $Ura3^+$ with a yeast genomic library cloned into multicopy vector YEp24 (5). About 8,000 transformants were replica plated onto synthetic complete medium lacking uracil and irradiated with 30 J of UV per m^2. Two UV-resistant clones were obtained, and the corresponding clones from the unirradiated master plate were transferred to synthetic complete medium supplemented with 5-fluoroorotic acid to promote plasmid loss (4). In both cases, a Ura^- phenotype was concomitant with the loss of UV resistance, indicating that the acquired UV resistance was plasmid borne. Plasmids obtained from yeast cells were propagated in *E. coli* DH5α. Restriction analysis of plasmids pBM102 and pBM104, isolated from the two UV-resistant clones, revealed that they contain two different DNA inserts of 10.5 and 11 kb, respectively. Plasmids pBM102 and pBM104 were introduced into *rad5-1* and *mms19-1* single mutant strains, and the UV sensitivity of the transformants was determined by the spot test as described previously (29). While plasmid pBM102 fully complemented the *rad5-1* mutation but did not confer any UV resistance on an *mms19-1* mutant strain, plasmid pBM104 fully complemented the UV and MMS sensitivities of an *mms19-1* mutant but did not increase UV resistance of *rad5-1* strains.

DNA sequencing. DNA fragments obtained by digestion with various restriction enzymes were cloned into M13mp18 and M13mp19. The nucleotide sequence of both strands of the *MMS19* gene was determined by the chain termination method (34) with deoxyadenosine 5′-(α-[^{35}S]thio)triphosphate (3).

Generation of genomic deletion mutations. Various *RAD* genes in isogenic yeast strains were deleted by replacing all or parts of the open reading frame (ORF) with the yeast *URA3* or *LEU2* gene by the one-step gene disruption method. Genomic deletions of the *RAD52* gene in strains DBY747 (*MAT*α *his3-*Δ*1 leu2-3,112 trp1-289 ura3-52*) and DBY747/19Δ (DBY747 made *mms19*Δ*::LEU2*$^+$) were generated by transforming these strains with a 3.3-kb *Bam*HI fragment of pSM22 in which the *Bgl*II-*Cla*I fragment in the *RAD52* ORF had been replaced by the *URA3* gene. The *RAD1* gene was replaced by the *URA3* gene from position −212 to +3853 in strain DBY747/19Δ (33). The *RAD6* gene in strain DBY747/19Δ, from position −43 to +565, was replaced by the *URA3* gene by transformation with *Bam*HI- and *Hin*dIII-digested plasmid pDG47, which contains the *URA3* gene flanked by *RAD6* nontranslated sequences. Deletion of each *RAD* gene was confirmed by testing of allelism with known *rad* mutations. Genomic deletion mutations of *MMS19* were constructed as described in the Fig. 3 legend.

UV irradiation and determination of sporulation efficiency. Yeast cells containing plasmids were grown to mid-exponential phase in liquid synthetic complete medium selective for the given plasmid harbored by the particular strain. Cells were washed, diluted, plated onto selective synthetic complete solid medium, and UV irradiated.

After 5 days of incubation at 30°C in liquid sporulation medium, sporulation efficiency was determined by microscopic examination of cells and counting with a hemacytometer.

Antibody production. Plasmid pMMS19.4, used for overexpressing Mms19 protein in *E. coli* for use as an antigen, was created by ligating an 800-bp *Spe*I-*Eco*RI fragment from the *MMS19* gene into the *Xba*I and *Eco*RI sites of pBJ63, thereby fusing amino acid residues 872 to 1032 of the Mms19 protein to the 116 amino-terminal residues of the *E. coli* rho protein plus 78 amino acid residues at the carboxyl terminus of the rho protein. Following induction by nalidixic acid treatment of *E. coli* cells harboring pMMS19.4, the insoluble rho-Mms19 fusion protein was purified by preparative sodium dodecyl sulfate-polyacrylamide gel electrophoresis (SDS-PAGE) and injected into New Zealand White rabbits. Antibodies were affinity purified with the rho-Mms19 fusion protein coupled to cyanogen bromide-activated Sepharose 4B as the affinity matrix. Purified anti-Mms19 antibodies were used for Western blots and, when coupled to protein A-agarose beads, for immunoprecipitation, as described previously (1).

Purification of Mms19 protein. Mms19 protein was purified from yeast strain LY2 (*MAT*α *leu2-3,112 gal1 reg1-501 pep4-3 ura3-52 trp1*Δ *prb112*) harboring plasmid pMMS19.7, in which the *MMS19* gene is under the control of the *GAL1-10-PGK* promoter, resulting in overexpression of Mms19 protein. Overnight cultures were grown in synthetic complete medium lacking leucine, inoculated into YPD medium containing 1% galactose, and grown for 13 h to a density of approximately 5×10^7 cells per ml. The cells were collected by centrifugation, washed once with distilled water, and stored at −70°C. The frozen cell paste (45 g) was thawed and then suspended (3 ml/g) in lysis buffer (50 mM Tris-HCl [pH 7.5], 100 mM NaCl, 5 mM dithiothreitol, 1 mM EDTA, 5% glycerol), and the cell suspension was lysed by passage through a French press. The lysate was clarified by centrifugation at 34,000 rpm in a Beckman Ty35 rotor for 1 h. Mms19 protein was precipitated from the cleared lysate by adding ammonium sulfate to 40% saturation (0.24 g/ml). The ammonium sulfate precipitate was dissolved in 30 ml of buffer A (same as lysis buffer but with 1 mM dithiothreitol and 0.1 mM EDTA), loaded onto a Q Sepharose Fast Flow column (2.5 by 10 cm), and eluted with a 500-ml 0.1 to 0.5 M NaCl gradient in buffer A. The fractions containing Mms19 protein were identified by immunoblotting,

pooled, and precipitated with ammonium sulfate (0.24 g/ml). The resulting pellet was dissolved in 2.5 ml of buffer B (10 mM KPO_4 [pH 6.5], 50 mM potassium acetate, 1 mM dithiothreitol), applied onto a Bio-Gel HT hydroxyapatite column (1.5 by 8 cm), and eluted with a 75-ml gradient of potassium phosphate (10 to 300 mM) in buffer B. The fractions containing Mms19 protein were then pooled (12 ml), dialyzed against buffer A, concentrated in a Centriprep-30 concentrator (Amicon) to 4 ml, and fractionated in a Mono Q (HR5/5) column with a 22.5-ml 0.1 to 0.5 M NaCl gradient in buffer A. The fractions containing Mms19 protein were pooled and concentrated in a Centricon-30 concentrator to 2.1 mg/ml. The yield of Mms19 protein with purity greater than 95% (see Fig. 8A, lane 6) was 10 mg.

Purification of TFIIH. TFIIH was purified from yeast strain YPH/TFB1.6HIS as described previously (11, 38). Briefly, extract was subjected to fractionation in columns of Bio-Rex 70, DEAE Sephacel, and hydroxyapatite. The TFIIH peak from hydroxyapatite was dialyzed and mixed with nickel-nitrilotriacetic acid-agarose to bind TFIIH through the 6-histidine tag on Tfb1 protein. The combined 40 and 100 mM imidazole eluates, which contained the bulk of TFIIH, were further fractionated in Mono S and Mono Q. As judged by silver staining following SDS-PAGE, the Mono Q TFIIH pool of greater than 95% purity contained stoichiometric amounts of Rad3, Rad25, Tfb1, Ssl1, p38, and p55 (12).

Pol II-dependent transcription in *MMS19* and *mms19*Δ strains. To examine Pol II-dependent transcription, extracts (200 μg of protein) prepared as described previously (12, 13) from wild-type and *mms19*Δ yeast strains, with or without pretreatment at 37°C for 5 min, were incubated, with the DNA template pSL187 containing the *CYC1* TATA element placed upstream of a 400-bp G-less cassette, at 25°C for the times indicated in Fig. 7. The reaction mixture was treated with RNase T_1 and deproteinized, and the RNA transcripts were precipitated at −70°C with ethanol and yeast tRNA as the carrier. The transcripts were dissolved in loading buffer (80% formamide, 0.1% Tris-borate-EDTA, 0.01% xylene cyanol FF, 0.01% bromophenol blue) and electrophoresed in a 4% acrylamide–7 M urea gel. The ^{32}P-labeled transcripts were visualized by autoradiography of dried gels.

Nucleotide sequence accession number. The GenBank accession number for the *MMS19* sequence is U70559. The *MMS19* sequence appears in the completed yeast genome sequence on chromosome 9.

RESULTS

Cloning and sequence analysis of the *MMS19* gene. The *MMS19* gene was cloned by complementing the UV sensitivity of the *mms19-1* mutation, using a yeast recombinant plasmid library in YEp24 as described in Materials and Methods. The initial 11-kb DNA insert was subcloned to localize the *mms19*-complementing activity to an ~4.2-kb *Eco*RV-*Eco*RI DNA fragment. That we had cloned *MMS19* was verified by allelism of the *mms19*Δ mutation with the *mms19-1* point mutation (see below). Nucleotide sequence determination of the ~4.2-kb *Eco*RV-*Eco*RI DNA fragment reveals one large ORF starting with the ATG initiation codon at position +1 and terminating with the TAA stop codon at position +3097 (Fig. 1). This ORF encodes a protein of 1,032 residues which has a predicted M_r of 117,912, which contains 12.2% acidic (aspartate and glutamate) and 12.1% basic (arginine, lysine, and histidine) amino acids, and which has a pI of 5.72.

Between residues 588 and 880, Mms19 protein contains a leucine-rich motif (LRM) of 15 tandem repeats (Fig. 2A). These LRM repeats are found in a variety of proteins that make up an LRM superfamily, and they vary in length from 22 to 29 amino acids. The LRM repeats are known to be involved in specific protein-protein interactions (see Discussion). The LRM repeat unit in Mms19 conforms most closely to the 22-amino-acid residue repeat in the *Schizosaccharomyces pombe* $sds22^+$ protein (28). This sequence has hydrophobic residues (usually Leu) at positions 3, 6, 12, 14, 19, and 22 with an invariant Asn residue at position 17 of the repeat, and it differs from longer LRM repeat units in lacking a proline residue at the beginning of each tandem repeat. Bestfit analysis of Mms19 and $sds22^+$ indicates that the homology between the two proteins is restricted to the LRM region (Fig. 2B). Aside from the LRM region, Mms19 shows no significant homology to proteins in the various data banks.

Assignment of *MMS19* to epistasis groups for UV repair. To define the biological roles of *MMS19*, we generated a genomic deletion mutation of this gene wherein the *MMS19* ORF from position +283 to +2931 was replaced by the yeast *LEU2* gene (Fig. 3). As expected from previous studies with the *mms19-1* mutant, the *mms19*Δ mutation caused sensitivity to MMS (data not shown) and to UV. The UV sensitivity of the *mms19*Δ mutant, however, is more pronounced than that of the *mms19-1* mutant (Fig. 4). The *mms19*Δ mutation is fully complemented by the *MMS19* gene carried on a low-copy yeast *CEN* plasmid, pBM205 (Fig. 4 and 6 and data not shown). To verify that we had cloned *MMS19*, we performed allelism tests of the *mms19*Δ mutation with the *mms19-1* mutation. As expected, the *mms19-1*/*mms19*Δ diploids displayed UV sensitivity, MMS sensitivity, and methionine auxotrophy (see below), indicating that the cloned gene was *MMS19*.

Genes belonging to three epistasis groups function in the repair of UV damage in *S. cerevisiae* (31). Those in the *RAD3* epistasis group are required for the removal of UV damage by NER, those in the *RAD6* epistasis group play a role in mutagenic and nonmutagenic postreplicative bypass of UV lesions by nonrecombinational means, and those in the *RAD52* group function in recombinational repair. To determine whether *MMS19* functions only in NER or whether it also affects other repair pathways, we performed epistasis analysis of the *mms19*Δ mutation with the *rad1*Δ mutation (defective in NER), the *rad6*Δ mutation (defective in postreplicative bypass), and the *rad52*Δ mutation (defective in recombinational repair). As shown in Fig. 5A, the UV sensitivity of the *rad1*Δ mutant is much greater than that of the *mms19*Δ mutant, and the UV sensitivity of the *mms19*Δ *rad1*Δ double mutant is the same as that of the *rad1*Δ single mutant. These results indicate an epistatic interaction between the *rad1*Δ and *mms19*Δ mutations. The *mms19*Δ *rad6*Δ double mutant, however, is much more UV sensitive than the *rad6*Δ single mutant (Fig. 5B). The synergistic increase in UV sensitivity of the *mms19*Δ *rad6*Δ mutant over that of the single mutants suggests that *MMS19* does not function in the *RAD6* repair pathway. Interestingly, the *mms19*Δ mutation shows epistasis with the *rad52*Δ mutation (Fig. 5C), suggesting a role of *MMS19* in the *RAD52*-dependent repair pathway as well.

Effects of the *mms19*Δ mutation on growth, methionine biosynthesis, and sporulation. The *mms19*Δ mutation affects cell growth adversely. At 30°C, growth is retarded, and *mms19*Δ cells do not grow at 37°C (Fig. 6A and B). At the restrictive temperature, mutants defective in DNA replication arrest as large budded cells (6), whereas those with a defect in Pol II transcription do not arrest uniformly at any cell cycle stage. Microscopic examination of *mms19*Δ cells held at 37°C did not reveal significant accumulation of cells at any cell cycle stage.

To examine if the *mms19*Δ mutation might affect the transcription of some specific genes, we tested the growth of the *mms19*Δ mutant at 30°C on synthetic complete medium lacking any one of the amino acids or the nucleic acid bases. Interestingly, we found that the *mms19*Δ mutant does not grow on medium lacking methionine (Fig. 6C and D). Examination of the *mms19-1* mutant revealed that it also is a methionine auxotroph.

To examine the effect of the *mms19*Δ mutation on sporulation, we constructed isogenic diploids which were either heterozygous or homozygous for the *mms19*Δ mutation and compared their rates of sporulation with that of an isogenic wild-type diploid strain. As shown in Table 1, in the homozygous *mms19*Δ/*mms19*Δ diploid, sporulation was severely reduced, while in the heterozygous *mms19*Δ/*MMS19* diploid, sporulation efficiency remained unaffected. Thus, the *mms19*Δ mutation causes a recessive sporulation defect.

FIG. 1. Nucleotide sequence of and predicted amino acid sequence encoded by the 4,149-bp DNA fragment containing the *MMS19* gene. Numbers on the left indicate nucleotide positions, relative to the translation start codon, and numbers on the right indicate amino acid positions. Various restriction endonuclease cleavage sites are underlined.

Defective Pol II transcription in *mms19*Δ mutant extracts. MMS19 could affect cell viability via an involvement in Pol II transcription. To test this idea directly, extracts were prepared (46) from isogenic wild-type and *mms19*Δ strains grown at 25°C, and their competence for Pol II transcription was determined with the template pSL187, which contains the yeast *CYC1* promoter and a 400 bp G-less region downstream of the promoter. As shown in Fig. 7A, extracts from the *mms19*Δ strain grown at 25°C carry out transcription at a level similar to that observed in extracts from isogenic wild-type cells. Importantly, while exposure to 37°C for 5 min had no effect on the transcriptional ability of the wild-type extract, this brief heat treatment completely inactivated the transcriptional competence of the *mms19*Δ extract (Fig. 7B). These studies indicate a thermolabile Pol II transcription defect in the *mms19*Δ mutant.

Purification of the Mms19 protein. To determine the manner in which Mms19 protein functions in transcription and NER and to examine its biochemical activities, the *MMS19* gene was overexpressed under the control of a *GAL1-10-PGK* fusion promoter (21), and its protein product was purified from *S. cerevisiae* (see Materials and Methods). As determined by Coomassie blue staining of a denaturing polyacrylamide gel, the purity of the resulting preparation is greater than 95% (Fig. 8A, lane 6). The identity of the Mms19 protein was verified by

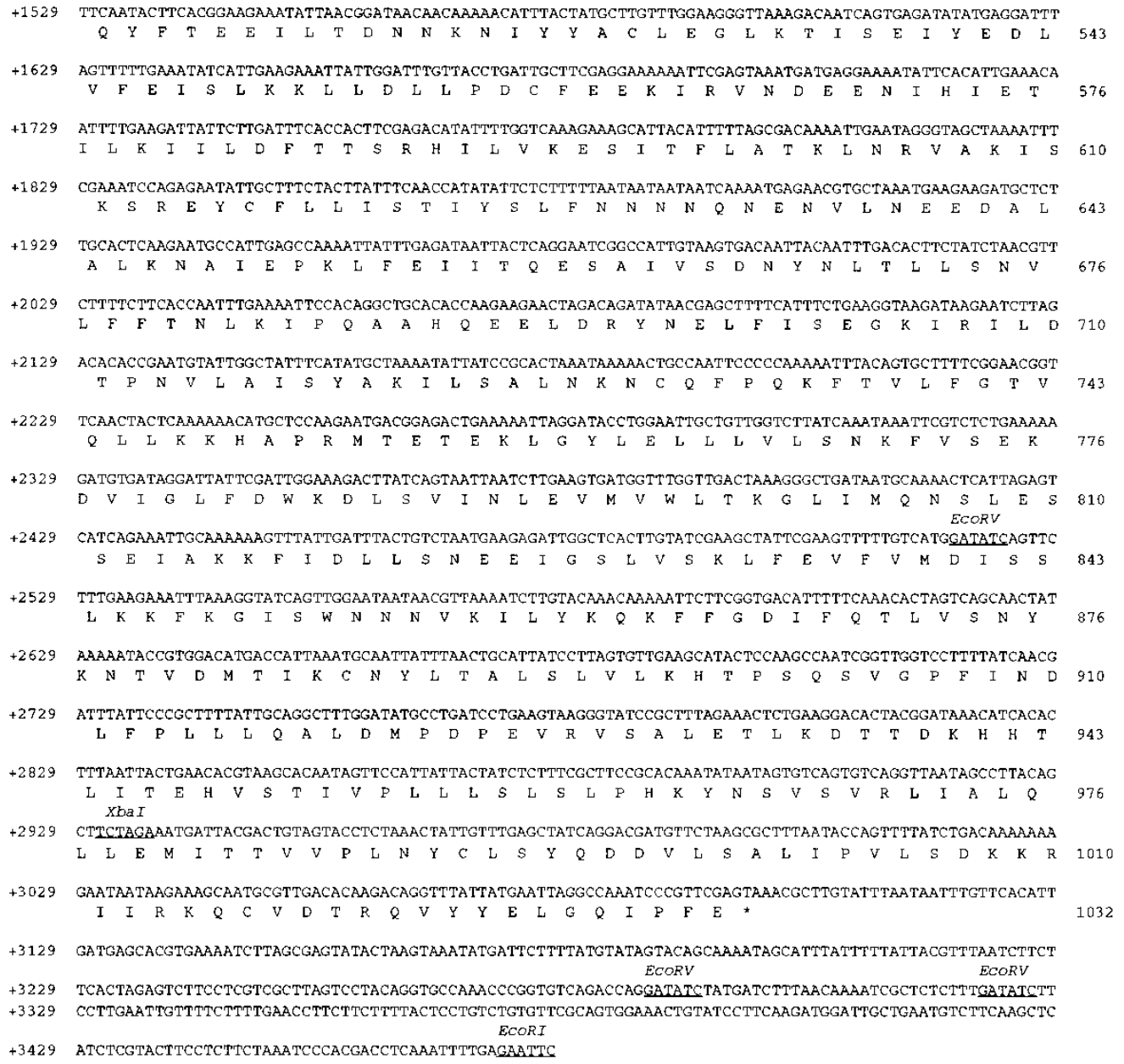

FIG. 1—*Continued.*

immunoblotting with affinity-purified Mms19-specific antibodies (Fig. 8B). In SDS-polyacrylamide gels, Mms19 migrates as a 104-kDa species.

Mms19 shows no strong homology to any other proteins currently in the databases, and it does not possess any known sequence motif suggesting an enzymatic function. Since the *MMS19* gene is involved in both DNA repair and transcription, we examined the purified Mms19 protein for single-stranded- and double-stranded-DNA binding activity using a filter binding assay. However, no DNA binding was observed.

The Mms19 protein is not physically associated with TFIIH. The dual involvement of the *MMS19* gene in NER and transcription is strongly reminiscent of the *RAD3* and *RAD25* genes, whose products are subunits of TFIIH. Therefore, it was of considerable interest to examine whether the Mms19 protein is also part of TFIIH. We performed immunoprecipitation from wild-type whole-cell yeast extract using affinity-purified antibodies directed against components of TFIIH (Tfb1 and Rad3). In these experiments, Mms19 protein did not coprecipitate with TFIIH, although two other components of TFIIH, i.e., Rad25 and Ssl1, were readily precipitated by the anti-Rad3 and anti-Tfb1 antibodies. Conversely, affinity-purified antibodies directed against the Mms19 protein also failed to coprecipitate TFIIH. In experiments employing purified Mms19 protein and ^{35}S-labeled TFIIH subunits produced in vitro with a coupled transcription-translation system, we again did not observe any interaction, as indicated by the lack of coimmunoprecipitation of Mms19 with the ^{35}S-labeled proteins. Taken together, our results indicate that Mms19 is not a component of TFIIH and that it does not interact with TFIIH physically.

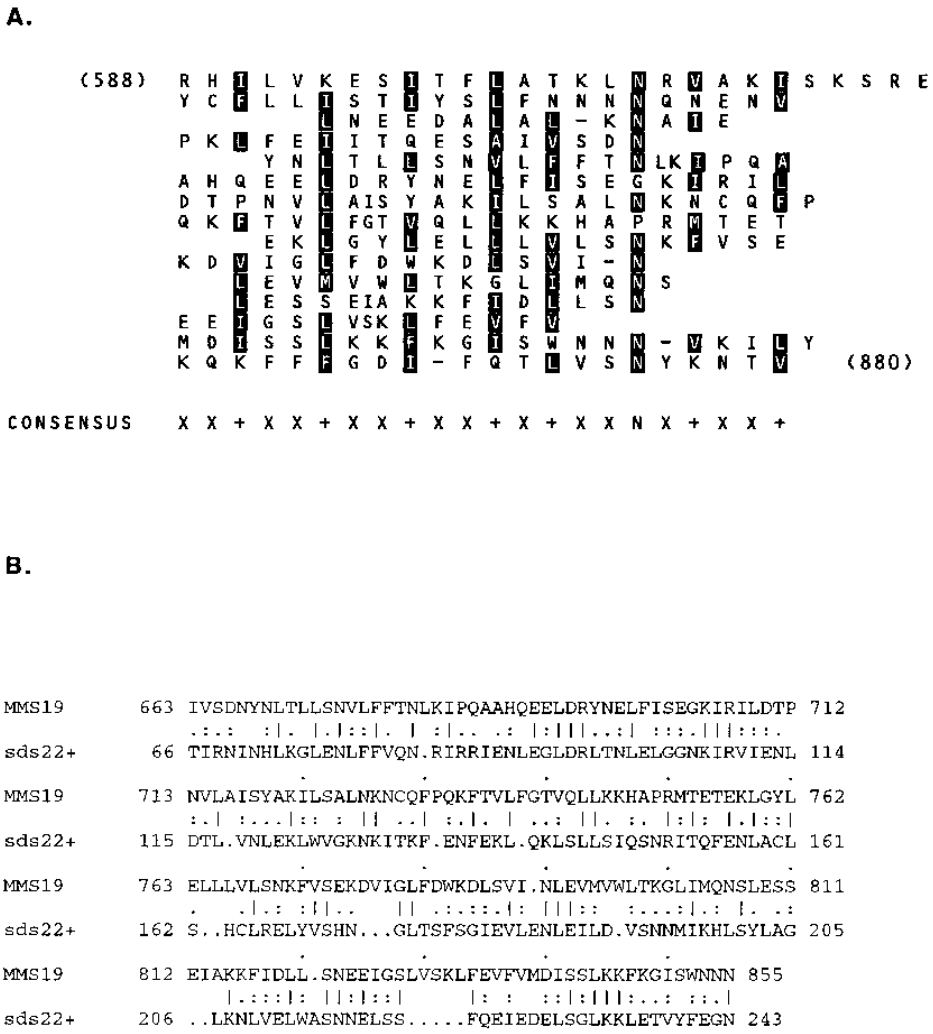

FIG. 2. LRMs in Mms19 protein. (A) The Mms19 protein contains an LRM with 15 repeats from amino acid residue 588 to 880. Amino acids in white lettering indicate those residues which conform to the consensus sequence for the LRM, where + refers to hydrophobic amino acids (most commonly Leu, Val, Ile, and Phe, but also Met and Ala), N is Asn, and X can be any amino acid. (B) Bestfit analysis of LRM repeats of Mms19 and *S. pombe* sds22$^+$ protein. The Bestfit program of the GCG computer sequence analysis package was used to align the LRM region of the Mms19 peptide to the sds22$^+$ protein sequence. Double dots between sequences indicate highly conserved residues; single dots between sequences indicate weakly conserved residues.

Consistent with this, when wild-type yeast extract was subjected to chromatographic fractionation in Bio-Rex 70 as described previously (16, 35, 38), Mms19 protein was absent from the 600 mM potassium acetate eluate that contained, in addition to TFIIH, the bulk of cellular core Pol II, of Pol II holoenzyme, and of various other transcription factors (35). Thus, it appears that the Mms19 protein is not a physical constituent of TFIIH or of any of the aforementioned components of the Pol II machinery.

TFIIH complements the transcriptional defect of the *mms19*Δ extract. We used the purified Mms19 protein to determine whether it complements the transcriptional defect of the *mms19*Δ mutant extract. Surprisingly, the addition of 100 ng (0.85 pmol) of Mms19 (Fig. 9, lane 4) or larger amounts (data not shown) did not restore transcriptional competence to heat-treated *mms19*Δ extract. We were then prompted to consider the possibility that Mms19 protein is not directly involved in transcription but rather that it affects the level or activity of transcription factors. Among the various Pol II transcription factors that might be influenced by Mms19, TFIIH represents an attractive candidate because, like Mms19, it is involved in both Pol II transcription and NER. To test our hypothesis directly, we examined transcription in heat-treated *mms19*Δ mutant extract supplemented with TFIIH purified to near homogeneity from yeast extract. The TFIIH preparation used in this work contained stoichiometric levels of the six subunits, Rad25, Rad3, Tfb1, Ssl1, p55, and p38 (11). As shown in Fig. 9, addition of 100 ng (0.25 pmol) of TFIIH to heat-treated *mms19*Δ extract restored nearly normal levels of transcriptional activity to the mutant extract (lane 3). These observations suggest that Mms19 exerts its effect on transcription via TFIIH.

Mms19 does not affect incision in the reconstituted system. Incision of UV-damaged DNA in *S. cerevisiae* has been reconstituted with highly purified protein components. In this system, dual incision of UV-damaged DNA is mediated by the combination of Rad14, the Rad4-Rad23 complex, Rad2, the Rad1-Rad10 complex, RPA, and TFIIH (11, 38). Addition of Mms19 protein to the reconstituted system, however, had no effect on the efficiency of the incision reaction (data not

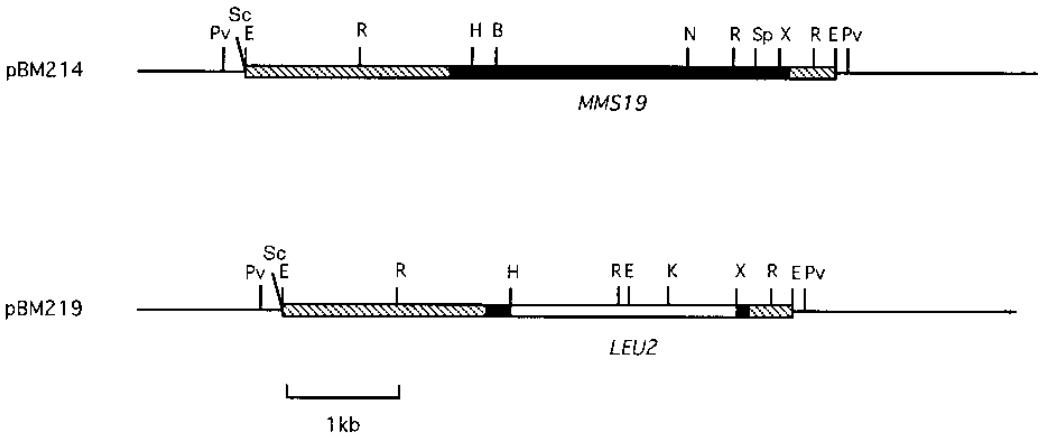

FIG. 3. Construction of a genomic deletion mutation of the *MMS19* gene. Plasmid pBM214 is a pUC19 derivative with the *Hin*dIII, *Sal*I, *Bam*HI, *Xba*I, and *Sma*I sites of the polylinker region removed. It harbors the 5.2-kb *Eco*RI fragment of pBM204, which contains the entire *MMS19* ORF and 5′- and 3′-flanking sequences of the *MMS19* gene. Plasmid pBM219 was constructed by replacing the 2.6-kb *Hin*dIII-*Xba*I fragment of pBM214, which contains most of the *MMS19* ORF, with a 2.0-kb *Hin*dIII/*Xba*I fragment of the yeast *LEU2* gene. Digestion of pBM219 with *Sac*I and *Pvu*II and transformation of an *MMS*$^+$ *leu2-3,112* strain to *LEU2*$^+$ generate *mms19*Δ mutants, in which all but the first 283 bp and the last 165 bp of the 3,096-bp *MMS19* ORF (Fig. 1) are replaced by the *LEU2* gene. Symbols for restriction sites: B, *Bam*HI; E, *Eco*RI; H, *Hin*dIII; K, *Kpn*I; N, *Nde*I; Pv, *Pvu*II; R, *Eco*RV; Sc, *Sac*I; Sp, *Spe*I; X, *Xba*I. The filled bar represents the *MMS19* ORF, the open bar represents the yeast *LEU2* gene, and the hatched bar represents the 5′- and 3′-flanking regions of the *MMS19* gene. Vector sequences (not drawn to scale) are represented by thin lines.

shown). Thus, the Mms19 protein does not affect the incision of UV-damaged DNA in the reconstituted NER system.

DISCUSSION

Studies with the *mms19*Δ mutation reported here indicate that *MMS19* affects, in addition to NER, other cellular processes. As expected from previously reported studies with the *mms19-1* mutation, the *mms19*Δ mutation shows epistasis with the *rad1*Δ mutation defective in NER. In addition, we find that the *mms19*Δ mutation interacts in an epistatic manner with the *rad52*Δ mutation defective in recombinational repair and that it impairs sporulation. These observations could be interpreted to suggest that *MMS19* affects the Rad52-dependent recombinational repair pathway and that the sporulation defect in *mms19*Δ homozygotes results from a deficiency in the *RAD52* recombination pathway in meiosis. The *mms19*Δ mutation also causes slow growth at 30°C, and growth ceases at 37°C. In addition, *mms19*Δ cells are methionine auxotrophs. In vitro transcriptional studies with the yeast *CYC1* promoter have indicated that *MMS19* has a role in Pol II transcription. Thus, *MMS19* is a multifunctional gene that affects NER, Pol II transcription, and possibly Rad52-dependent recombinational repair as well.

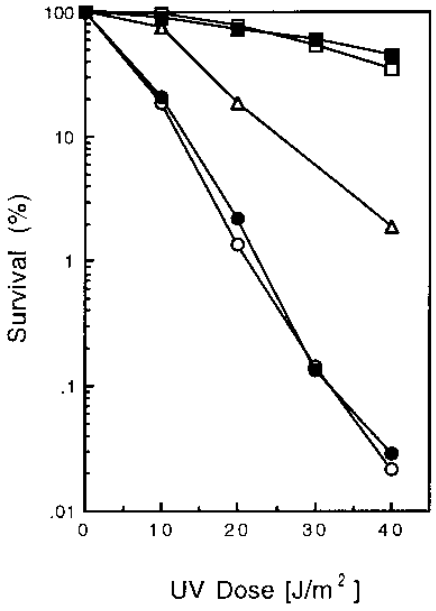

FIG. 4. UV sensitivity of the *mms19*Δ strain. Symbols: ■, DBY747 (wild type); △, LP2745-4B (*mms19-1*); ○, *mms19*Δ strain; ●, *mms19*Δ strain with *CEN* vector YCplac33; □, *mms19*Δ strain with pBM205, which carries *MMS19* on a yeast *CEN* plasmid. The *mms19*Δ mutation was generated in the DBY747 strain. Strains carrying plasmids were grown in complete medium lacking uracil for selection of plasmids.

Among the NER genes, *RAD3*, *RAD25*, and *MMS19* resemble one another in that they also affect Pol II transcription. However, unlike Rad3 and Rad25, Mms19 is not physically associated with TFIIH. We showed previously that the transcriptional defect in *rad3* and *rad25* mutant extracts can be corrected fully by the addition of purified Rad3 or Rad25 protein, respectively (12, 13), indicating a direct role of the Rad3 and Rad25 proteins in Pol II transcription. By contrast, Mms19 does not complement the thermolabile transcriptional defect of the *mms19*Δ extract, nor does it affect incision of UV-damaged DNA reconstituted from purified components. Thus, unlike Rad3 and Rad25, Mms19 appears to function in NER and transcription as an upstream regulatory element. The ability of purified TFIIH to complement the thermolabile transcriptional defect of the *mms19*Δ extract is consistent with the suggestion that the functional integrity of TFIIH is dependent upon Mms19. The compromised functional integrity of TFIIH would also be the basis of the NER deficiency in the *mms19* mutant.

Mms19 protein contains an LRM of 15 tandem repeats which resemble similar repeats in the *S. pombe* sds22$^+$ protein. Genetic studies have suggested that sds22$^+$ protein positively modulates the activity of one of the type 1 protein phosphatases (28). The regulatory subunit of mammalian type 2A protein phosphatase also contains an LRM, and LRMs have been identified in various other proteins, including adenylate cyclase

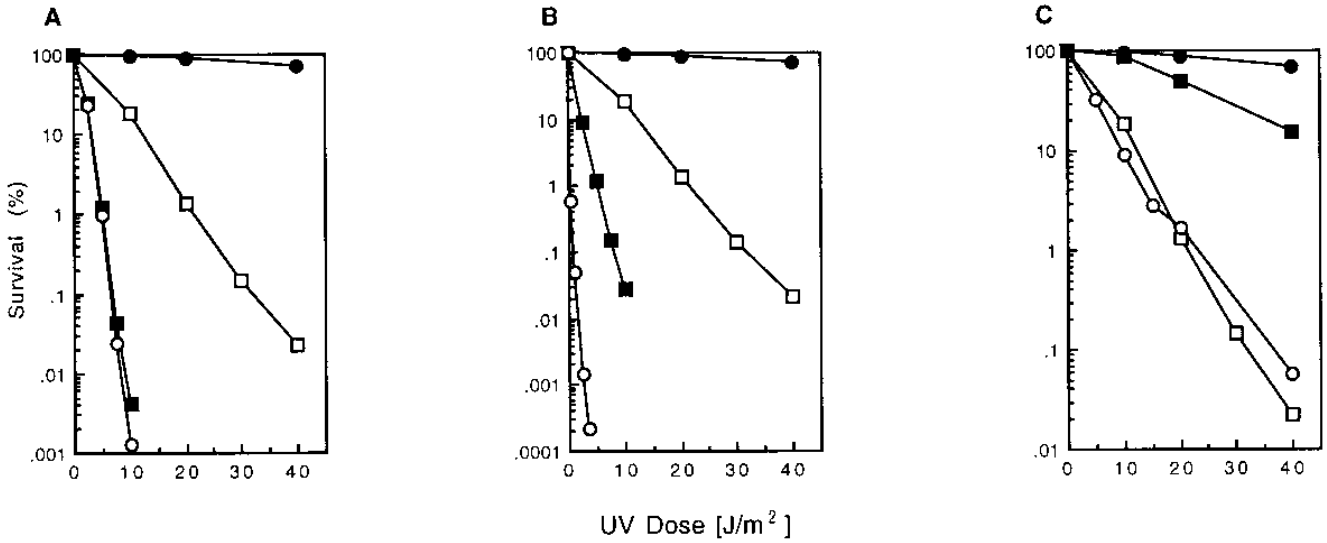

FIG. 5. Epistasis analysis of the *mms19*Δ mutation with various *rad* mutations. UV survival of isogenic *mms19*Δ and *rad*Δ strains derived from DBY747 is shown. ●, wild type; □, *mms19*Δ strain. (A) ■, *rad1*Δ strain; ○, *mms19*Δ *rad1*Δ strain; (B) ■, *rad6*Δ strain; ○, *mms19*Δ *rad6*Δ strain; (C) ■, *rad52*Δ strain; ○, *mms19*Δ *rad52*Δ strain. DBY747 and its derivative *mms19*Δ and *rad*Δ mutant strains were incubated in the dark for 3 to 6 days on YPD medium following UV irradiation.

and the platelet membrane receptor GP1bα. The leucine-rich repeats in adenylate cyclase mediate interaction with the Ras protein to activate adenylate cyclase function (47), and the repeats in the GP1bα receptor bind von Willebrand factor (23). The LRMs in Mms19 could also be involved in specific protein-protein interactions, and like $sds22^{+}$ and other proteins, Mms19 could act as a regulatory subunit in a protein complex that functions in signal transduction via protein phosphorylation or dephosphorylation. According to this scenario, Mms19 would affect NER and transcription by modulating the functional ability of TFIIH via post-translational modifications (Fig. 10). The involvement of Mms19 in sporulation and pos-

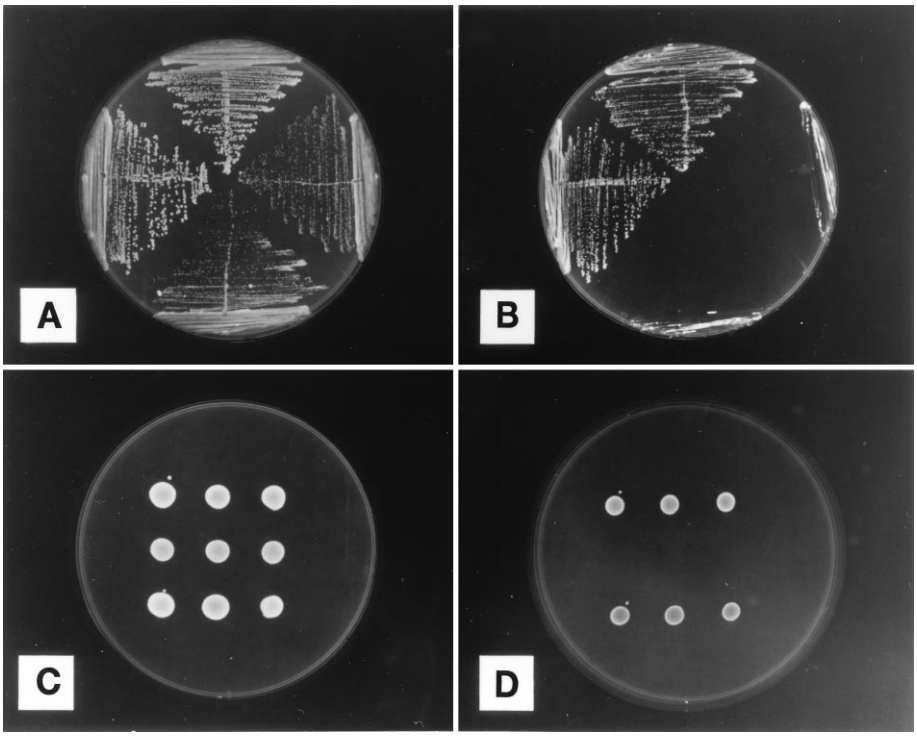

FIG. 6. The *mms19*Δ mutation causes conditional lethality and methionine auxotrophy. Cells were streaked onto complete medium and incubated for 48 h at 30°C (A) or 37°C (B). Strains in panels A and B: top, wild type; bottom, *mms19*Δ strain; right, *mms19*Δ strain with yeast vector YCplac33; left, *mms19*Δ strain with pBM205, which carries *MMS19* on a yeast *CEN* plasmid. Cells were transferred to synthetic complete medium (C) or synthetic complete medium lacking methionine (D), and plates were incubated for 2 days at 30°C. Strains in panels C and D: top row, wild type; middle row, *mms19*Δ strain; bottom row, *mms19*Δ strain with pBM205. The *mms19*Δ derivative of DBY747 was used in these experiments.

TABLE 1. Sporulation efficiency in isogenic *MMS19*/*MMS19*, *MMS19*/*mms19*Δ, and *mms19*Δ/*mms19*Δ diploids

Strain[a]	Genotype	% Sporulation[b]	Sporulation relative to wild-type strain
BM1507	*MMS19*/*MMS19*	49.4 ± 3.5	100
BM1519	*mms19*Δ/*MMS19*	47.1 ± 2.7	95
BM1520	*mms19*Δ/*mms19*Δ	2.5 ± 0.6	5

[a] Diploid BM1507 was made by crossing DBY745 (*MAT*α *ura3-52 leu2-3,112 ade1-100*) with Y428 (*MAT***a** *ura3-52 leu2-*Δ*98 trp1-*Δ*901 lys2-801 ade2-101*). To obtain BM1519, DBY745 was crossed with Y428/19Δ, which is Y428 made *mms19*Δ::*LEU2*, while BM1520 was constructed by crossing DBY745/19Δ with Y428/19Δ.

[b] Sporulation efficiency was determined from the proportion of asci among cells.

sibly in the Rad52 recombinational repair pathway might suggest that besides TFIIH, Mms19 modifies the activity of components involved in this recombination pathway as well (Fig. 10). Mutations in the *RAD52* group of genes confer a high degree of sensitivity to MMS, presumably because of an inability to repair MMS-induced DNA strand breaks by recombinational repair. An involvement of *MMS19* in the activation of recombinational proteins might underlie the MMS-sensitive phenotype of *mms19* mutants.

Mutations in TFIIH subunits can impair NER, transcription, or both processes simultaneously, and all three classes of mutations have in fact been identified in genes encoding the yeast TFIIH subunits Rad3 and Rad25 (12, 13, 31, 43). Mms19 represents the first protein factor shown to have a role in both NER and Pol II transcription, but in contrast to TFIIH, it does not act directly in these processes. Our findings with Mms19 may have an important bearing on human syndromes in which both NER and transcription are affected. Trichothiodystrophy, which is characterized by sulfur-deficient brittle hair, physical and mental retardation, and microcephaly, can be caused by mutations in *XPB* and *XPD* and also by mutations in genes other than any of the known *XP* genes (reviewed in reference 8). While a severe defect in the removal of UV damage results in XP, a deficiency in the transcription process could be the cause of trichothiodystrophy symptoms (15). We suggest that mutations in the human *MMS19* counterpart and in other functionally related genes will be found in syndromes with deficiencies in both NER and transcription and may be the cause of some trichothiodystrophy cases. Our work also highlights the possibility that complementation of the NER or transcription defect in a mutant extract by TFIIH does not necessarily reflect direct mutational inactivation of a subunit of TFIIH in that mutant, as mutational inactivation of an up-

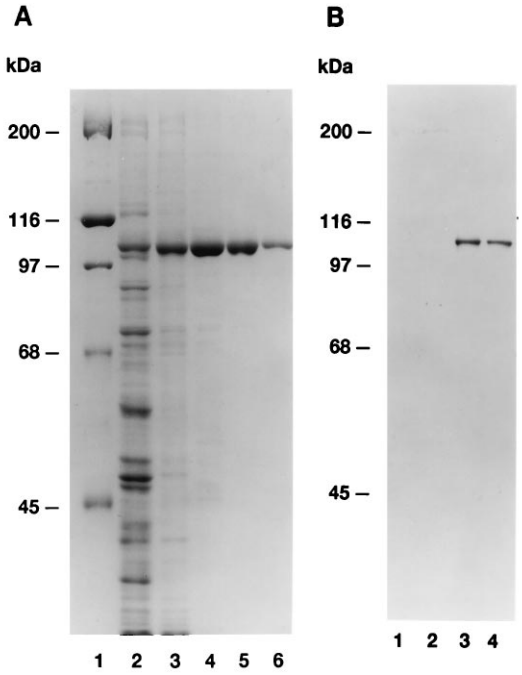

FIG. 8. Purification of Mms19 protein. (A) SDS-PAGE showing stages in the purification of Mms19 protein from yeast cells. Lane 1, molecular mass markers; lane 2, cleared lysate (100 μg of total protein); lane 3, Q Sepharose column load (20 μg); lane 4, hydroxyapatite column load (5 μg); lane 5, Mono Q column load (5 μg); lane 6, purified Mms19 protein pool (1 μg). (B) Immunoblot probed with Mms19-specific antibodies. Lane 1, extract from wild-type strain DBY747 (the level of Mms19 protein in wild-type cells is too low to be visualized under these conditions); lane 2, extract from *mms19*Δ strain; lane 3, extract from Mms19-overproducing cells; lane 4, purified Mms19 protein.

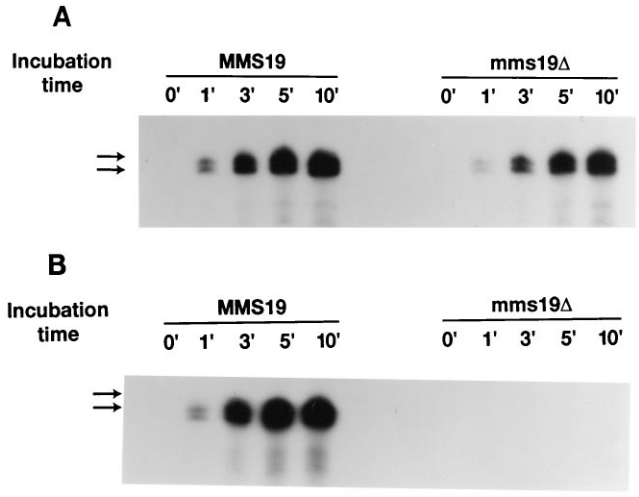

FIG. 7. Pol II transcription in *mms19*Δ extract is thermolabile. Extracts prepared from isogenic wild-type and *mms19*Δ cells were examined for Pol II-dependent transcriptional activity at 25°C for the times indicated without (A) or with (B) a 5-min pretreatment of the extracts at 37°C. Arrows indicate the 375 (top arrow)- and 350 (bottom arrow)-nucleotide transcripts. Transcription reactions were carried out and analyzed as described previously (12, 13).

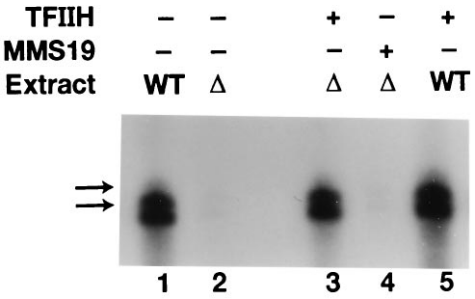

FIG. 9. TFIIH but not Mms19 alleviates the transcriptional defect of the *mms19*Δ extract. Wild-type (lanes 1 and 5) and *mms19*Δ (lanes 2 to 4) extracts were heated for 5 min at 37°C and examined for Pol II transcription after the addition of 0.1 μg of Mms19 protein (lane 4) or 0.1 μg of TFIIH (lanes 3 and 5). Transcription reactions were carried out and analyzed as described previously (12, 13). The arrows indicate the 375 (top arrow)- and 350 (bottom arrow)-nucleotide transcripts.

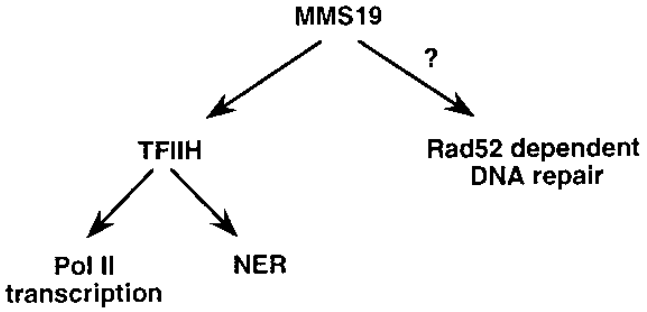

FIG. 10. The various roles of Mms19. It is proposed that Mms19 affects transcription and NER by modulating TFIIH activity. Epistasis analyses also suggest a possible role of Mms19 in modulating Rad52-dependent DNA repair.

stream regulatory element such as *MMS19* could affect the functional integrity of TFIIH.

ACKNOWLEDGMENTS

We are grateful to John Watkins for homology searches, for the identification of the LRM in Mms19, and for help with the preparation of the manuscript.

This work was supported by grants CA41261 from NCI, ES07061 from NIEHS, and DE-FGO3-93ER61706 from DOE, and by a postdoctoral fellowship to M.B. from the Deutscher Akademischer Austauschdienst.

REFERENCES

1. **Bailly, V., C. H. Sommers, P. Sung, L. Prakash, and S. Prakash.** 1992. Specific complex formation between proteins encoded by the yeast DNA repair and recombination genes *RAD1* and *RAD10*. Proc. Natl. Acad. Sci. USA **89:**8273–8277.
2. **Bardwell, A. J., L. Bardwell, A. E. Tomkinson, and E. C. Friedberg.** 1994. Specific cleavage of model recombination and repair intermediates by the yeast Rad1-Rad10 DNA endonuclease. Science **265:**2082–2085.
3. **Biggin, M. D., T. J. Gibson, and G. F. Hong.** 1983. Buffer gradient gels and ^{35}S label as an aid to rapid DNA sequence determination. Proc. Natl. Acad. Sci. USA **80:**3963–3965.
4. **Boeke, J. D., F. LaCroute, and G. R. Fink.** 1984. A positive selection for mutants lacking orotidine-5′-phosphate decarboxylase activity in yeast: 5-fluoro-orotic acid resistance. Mol. Gen. Genet. **197:**345–346.
5. **Carlson, M., and D. Botstein.** 1982. Two differentially regulated mRNA's with different 5′ ends encode secreted and intracellular forms of yeast invertase. Cell **28:**145–154.
6. **Culotti, J., and L. H. Hartwell.** 1971. Genetic control of the cell division cycle in yeast. III. Seven genes controlling nuclear division. Exp. Cell Res. **67:**389–401.
7. **Feaver, W. J., J. Q. Svejstrup, L. Bardwell, A. J. Bardwell, S. Buratowski, K. D. Gulyas, T. F. Donahue, E. C. Friedberg, and R. D. Kornberg.** 1993. Dual roles of a multiprotein complex from *S. cerevisiae* in transcription and DNA repair. Cell **75:**1379–1387.
8. **Friedberg, E. C., G. C. Walker, and W. Siede.** 1995. DNA repair and mutagenesis. ASM Press, Washington, D.C.
9. **Gietz, R. D., and A. Sugino.** 1988. New yeast-*Escherichia coli* shuttle vectors constructed with in vitro mutagenized yeast genes lacking six-base pair restriction sites. Gene **74:**527–534.
10. **Guzder, S. N., V. Bailly, P. Sung, L. Prakash, and S. Prakash.** 1995. Yeast DNA repair protein RAD23 promotes complex formation between transcription factor TFIIH and DNA damage recognition factor RAD14. J. Biol. Chem. **270:**8385–8388.
11. **Guzder, S. N., Y. Habraken, P. Sung, L. Prakash, and S. Prakash.** 1995. Reconstitution of yeast nucleotide excision repair with purified Rad proteins, replication protein A, and transcription factor TFIIH. J. Biol. Chem. **270:** 12973–12976.
12. **Guzder, S. N., H. Qiu, C. H. Sommers, P. Sung, L. Prakash, and S. Prakash.** 1994. DNA repair gene *RAD3* of *S. cerevisiae* is essential for transcription by RNA polymerase II. Nature (London) **367:**91–94.
13. **Guzder, S. N., P. Sung, V. Bailly, L. Prakash, and S. Prakash.** 1994. RAD25 is a DNA helicase required for DNA repair and RNA polymerase II transcription. Nature (London) **369:**578–581.
14. **Guzder, S. N., P. Sung, L. Prakash, and S. Prakash.** 1993. Yeast DNA repair gene *RAD14* encodes a zinc metalloprotein with affinity for ultraviolet damaged DNA. Proc. Natl. Acad. Sci. USA **90:**5433–5437.
15. **Guzder, S. N., P. Sung, S. Prakash, and L. Prakash.** 1995. Lethality in yeast of triochothiodystrophy (TTD) mutations in the human xeroderma pigmentosum group D gene. J. Biol. Chem. **270:**17660–17663.
16. **Guzder, S. N., P. Sung, L. Prakash, and S. Prakash.** 1996. Nucleotide excision repair in yeast is mediated by sequential assembly of repair factors and not by a pre-assembled repairosome. J. Biol. Chem. **271:**8903–8910.
17. **Habraken, Y., P. Sung, L. Prakash, and S. Prakash.** 1993. Yeast excision repair gene *RAD2* encodes a single-stranded DNA endonuclease. Nature (London) **366:**365–368.
18. **Habraken, Y., P. Sung, L. Prakash, and S. Prakash.** 1995. Structure-specific nuclease activity in yeast nucleotide excision repair protein Rad2. J. Biol. Chem. **270:**30194–30198.
19. **Ito, H., Y. Fukuda, K. Murata, and A. Kimura.** 1983. Transformation of intact yeast cells treated with alkali cations. J. Bacteriol. **153:**163–168.
20. **Johansen, T.** 1988. Cloning of specific restriction fragments directly from low-melting point agarose gels. DNA Protein Eng. Tech. **1:**57–59.
21. **Kingsman, S. M., D. Cousens, C. A. Stanway, A. Chambers, M. Wilson, and A. J. Kingsman.** 1990. High-efficiency yeast expression vectors based on the promoter of the phosphoglycerate kinase gene. Methods Enzymol. **185:**329–341.
22. **Kraemer, K. H., C. N. Parris, E. M. Gozukara, D. D. Levy, S. Adelberg, and M. M. Seidman.** 1993. Human DNA repair-deficient diseases: clinical disorders and molecular defects. Alfred Benzon Symp. **35:**15–22.
23. **Lopez, J. A., D. W. Chung, K. Fujikawa, F. S. Hagen, T. Papayannopoulou, and G. J. Roth.** 1987. Cloning of the α chain of human platelet glycoprotein Ib: a transmembrane protein with homology to leucine-rich α2-glycoprotein. Proc. Natl. Acad. Sci. USA **84:**5616–5619.
24. **Maniatis, T., E. F. Fritsch, and J. Sambrook.** 1982. Molecular cloning: a laboratory manual. Cold Spring Harbor Laboratory, Cold Spring Harbor, N.Y.
25. **Miller, R. D., L. Prakash, and S. Prakash.** 1982. Genetic control of excision of *Saccharomyces cerevisiae* interstrand DNA cross-links induced by psoralen plus near-UV light. Mol. Cell. Biol. **2:**939–948.
26. **Mu, D., D. S. Hsu, and A. Sancar.** 1996. Reaction mechanism of human DNA repair excision nuclease. J. Biol. Chem. **271:**8285–8294.
27. **Mu, D., C.-H. Park, T. Matsunaga, D. S. Hsu, J. T. Reardon, and A. Sancar.** 1995. Reconstitution of human DNA repair excision nuclease in a highly defined system. J. Biol. Chem. **270:**2415–2418.
28. **Ohkura, H., and M. Yanagida.** 1991. S. pombe gene *sds22+* essential for a midmitotic transition encodes a leucine-rich repeat protein that positively modulates protein phosphatase-1. Cell **64:**149–157.
29. **Prakash, L., and S. Prakash.** 1977. Isolation and characterization of MMS-sensitive mutants of *Saccharomyces cerevisiae*. Genetics **86:**33–55.
30. **Prakash, L., and S. Prakash.** 1979. Three additional genes involved in pyrimidine dimer removal in *Saccharomyces cerevisiae*: *RAD7*, *RAD14* and *MMS19*. Mol. Gen. Genet. **176:**351–359.
31. **Prakash, S., P. Sung, and L. Prakash.** 1993. DNA repair genes and proteins of *Saccharomyces cerevisiae*. Annu. Rev. Genet. **27:**33–70.
32. **Qiu, H., E. Park, L. Prakash, and S. Prakash.** 1993. The *Saccharomyces cerevisiae* DNA repair gene *RAD25* is required for transcription by RNA polymerase II. Genes Dev. **7:**2161–2171.
33. **Reynolds, P., L. Prakash, and S. Prakash.** 1987. Nucleotide sequence and functional analysis of the *RAD1* gene of *Saccharomyces cerevisiae*. Mol. Cell. Biol. **7:**1012–1020.
34. **Sanger, F., S. Nicklen, and A. R. Coulson.** 1977. DNA sequencing with chain-terminating inhibitors. Proc. Natl. Acad. Sci. USA **74:**5463–5467.
35. **Sayer, M. H., H. Tschochner, and R. D. Kornberg.** 1992. Reconstitution of transcription with five purified initiation factors and RNA polymerase II from *Saccharomyces cerevisiae*. J. Biol. Chem. **267:**23376–23382.
36. **Sherman, F., G. R. Fink, and J. B. Hicks.** 1986. Methods in yeast genetics: a laboratory manual. Cold Spring Harbor Laboratory, Cold Spring Harbor, N.Y.
37. **Sung, P., V. Bailly, C. Weber, L. H. Thompson, L. Prakash, and S. Prakash.** 1993. Human xeroderma pigmentosum group D gene encodes a DNA helicase. Nature (London) **365:**852–855.
38. **Sung, P., S. N. Guzder, L. Prakash, and S. Prakash.** 1996. Reconstitution of TFIIH and requirement of its DNA helicase subunits, Rad3 and Rad25, in the incision step of nucleotide excision repair. J. Biol. Chem. **271:**10821–10826.
39. **Sung, P., D. Higgins, L. Prakash, and S. Prakash.** 1988. Mutation of lysine-48 to arginine in the yeast RAD3 protein abolishes its ATPase and DNA helicase activities but not the ability to bind ATP. EMBO J. **7:**3263–3269.
40. **Sung, P., L. Prakash, S. W. Matson, and S. Prakash.** 1987. RAD3 protein of *Saccharomyces cerevisiae* is a DNA helicase. Proc. Natl. Acad. Sci. USA **84:**8951–8955.
41. **Sung, P., L. Prakash, S. Weber, and S. Prakash.** 1987. The *RAD3* gene of *Saccharomyces cerevisiae* encodes a DNA-dependent ATPase. Proc. Natl. Acad. Sci. USA **84:**6045–6049.
42. **Sung, P., P. Reynolds, L. Prakash, and S. Prakash.** 1993. Purification and characterization of the *Saccharomyces cerevisiae* RAD1/RAD10 endonucle-

ase. J. Biol. Chem. **268:**26391–26399.
43. **Sweder, K., and P. C. Hanawalt.** 1994. The COOH terminus of suppressor of stem loop (*SSL2*/*RAD25*) in yeast is essential for overall genomic excision repair and transcription-coupled repair. J. Biol. Chem. **269:**1852–1857.
44. **Tomkinson, A. E., A. J. Bardwell, L. Bardwell, N. J. Tappe, and E. C. Friedberg.** 1993. Yeast DNA repair and recombination proteins Rad1 and Rad10 constitute a single-stranded-DNA endonuclease. Nature (London) **362:**860–862.
45. **Watkins, J. F., P. Sung, L. Prakash, and S. Prakash.** 1993. The *Saccharomyces cerevisiae* DNA repair gene *RAD23* encodes a nuclear protein containing a ubiquitin-like domain required for biological function. Mol. Cell. Biol. **13:**7757–7765.
46. **Woontner, M., P. A. Wade, J. Bonner, and J. A. Jaehning.** 1991. Transcriptional activation in an improved whole-cell extract from *Saccharomyces cerevisiae*. Mol. Cell. Biol. **11:**4555–4560.
47. **Young, D., M. Riggs, J. Field, A. Vojtek, D. Broek, and M. Wigler.** 1989. The adenylyl cyclase gene from *Schizosaccharomyces pombe*. Proc. Natl. Acad. Sci. USA **86:**7989–7993.